A complementary numerical and experimental study of a helium plasma jet for E.coli inactivation

A. Obrusník[1], K. Arjunan[2], S. Ptasinska[2,3], L. Zajíčková[1,4]

[1]*Department of Physical Electronics, Faculty of Science, Masaryk University, Brno, Czech Republic*
[2]*Radiation Laboratory, University of Notre Dame, Notre Dame, 46556 IN, USA*
[3]*Department of Physics, University of Notre Dame, Notre Dame, 46556 IN, USA*
[4]*Plasma Technologies at CEITEC, Masaryk University, Brno, Czech Republic*
adamobrusnik@physics.muni.cz

This contribution presents a two-dimensional numerical model of the gas dynamics, gas mixing and afterglow chemistry in a high-frequency atmospheric-pressure plasma jet for E.coli inactivation. The numerical modelling is combined with biomedical experiments in order to better understand the afterglow chemistry and the importance of gas dynamics and mixing in this plasma jet.

1. Introduction

Atmospheric-pressure plasma jets (APPJs) ignited in a noble gas and operating in ambient atmosphere have been utilized in the past years in a number of promising biomedical applications including wound healing and cancer treatment [1,2]. Since these plasma sources are very efficient in producing reactive oxygen species (ROS) and reactive nitrogen species (RNS), they are a very promising tool for inactivating microorganisms on surfaces [3]. Sterilization using APPJ plasmas is free of the disadvantages of the conventional sterilization methods, such as autoclaving or hydrogen peroxide treatment, because it does not require high temperatures and produces much smaller amounts of toxic by-products. This makes it a very promising alternative.

Despite numerous studies, the mechanism of interaction of APPJ with biological systems still remains poorly understood. To provide deeper insight into the mechanism, we started developing a two-dimensional numerical model describing the production and transport of various radical species in the afterglow of an atmospheric pressure helium jet. The results of this model are correlated with investigations of E.coli inactivation by this plasma jet. By doing so, we aim to identify which reactive species play an important role in this application.

The model is implemented using the COMSOL Multiphysics simulation platform, which discretizes differential equations using the finite element method.

2. Experimental

The discharge described in this work is a dielectric barrier discharge-type plasma jet. The plasma is ignited in helium or helium/oxygen mixtures using pulsed DC voltage with the pulse length of 100 µs and the frequency of 1.5 kHz. The voltage at the powered electrode was measured to be 11 kV. Details of the experimental set-up and characteristics of APPJ can be found in [4]

3. Model

The model consists of two parts, the *background gas dynamics* part describes the gas flow and mixing of the background gases (i.e., helium and air) and the *afterglow chemistry* part which describes the production and loss of selected radicals and their transport through the effluent.

All the equations are solved in two-dimensional axially symmetrical geometry (see figure 1), therefore the model is capable of providing spatially-resolved fluxes of radicals to the surface.

The computational geometry consists of a capillary tube with a diameter of 5 mm and a Petri dish with the diameter of 10 cm. The distance of the Petri dish from the jet outlet varies from 0.5 cm to 2.5 cm.

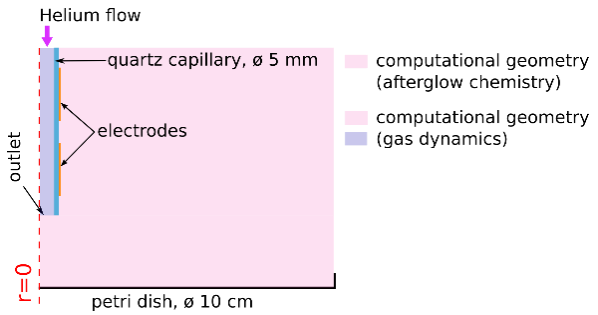

Figure 1: The computational geometry. The gas dynamics is solved for both inside and outside the capillary (pink+blue area), the afterglow chemistry only outside (pink area)

2.1. Background gas dynamics

The gas dynamics part of the model describes the flow and mixing of the background gases – helium and ambient air – with air being considered a single component. The model solves the Navier-Stokes equations for laminar flow (Reynolds number around 200) for the helium-air mixture. In the Navier-Stokes equations, the mixture density and viscosity are considered functions of the local gas composition and the viscosity is calculated using Wilke's mixture rules [5].

The local gas composition is obtained by solving a diffusion equation for the binary helium-air mixture. Since the helium-air mixture is non-dilute, the diffusion model that is employed uses fluxes in the Fick form with diffusion coefficient calculated using mixture rules from Chapman-Enskog binary diffusion coefficients.

2.2 Afterglow chemistry

The afterglow chemistry model includes diffusion equations that are solved for selected radicals outside the capillary (see figure 1). The diffusion equation is, in this case, solved in the form

$$\nabla \cdot (D_i \nabla c_i + \mathbf{u} c_i) = R_i \qquad (1)$$

where c_i is the molar concentration of species *i*, **u** is the mixture velocity obtained from the *background gas dynamics* model, R_i is the source term and D_i is the diffusion coefficient. The diffusion coefficients are, again, calculated from binary diffusion coefficients using the mixture rules and are, therefore also a function of the background gas composition. It is assumed that the radicals produced in the afterglow do not change the gas dynamics. This is a reasonable assumption since the mole fractions of the radical species do not exceed 10^{-4}. The afterglow model currently contains 55 reactions including the following radical species: $He^*, O_2^+, O_2(^1D), O, O_3, H_2O^+, H, HO_2, OH, N_2^+, N^+, N, NO, NO_2$.

The species and reactions were chosen based on especially the works of Murakami et al. [6] and a book by Capitelli et al. [7]. These references contain very extensive reaction schemes of dozens species and thousands reactions. Such complex reaction schemes would not be feasible in a 2D model but luckily, the referenced publications also contain assessment of the importance of individual reactions and identify the most important ones.

The afterglow model is constrained only by Dirichlet-type boundary conditions. At the remote boundaries, it is assumed that all the radicals and

Figure 2: E. coli inactivation area (dark) for the jet-helium distance of 1.5 cm and helium flow rate of 5.5 slm in a Petri dish with 10 cm diameter.

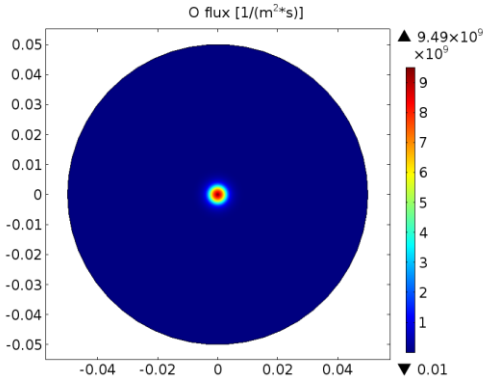

(a) Atomic oxygen radical

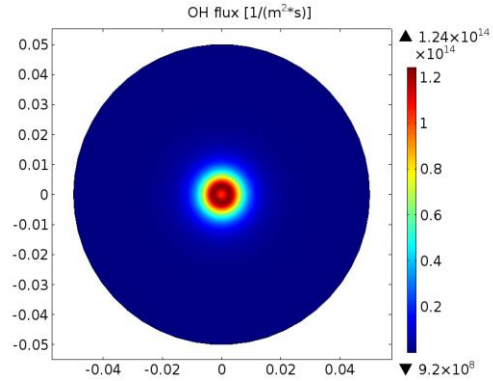

(b) Hydroxyl radical

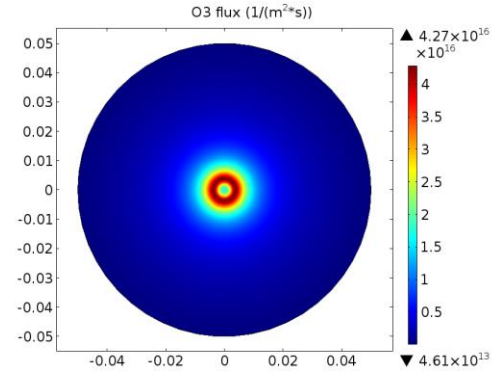

(c) Ozone

Figure 3: Fluxes of various radicals in [1/m^{3}s] to the Petri dish obtained from the numerical model. The diameter of the Petri dish is 10 cm

non-ground state species have recombined and their concentrations are set to zero. At the inlet, the concentration of the helium metastable He* is set to

$$c_{He} = 4 \cdot 10^{15}\ [m^{-3}] \cdot N_A$$

where N_A is the Avogadro number and the number density of $4 \cdot 10^{15}\ m^{-3}$ was estimated based on literature [8].

This choice of boundary conditions follows from an assumption that ionization and dissociation outside of the capillary tube is induced exclusively by helium metastables. Given the configuration of the driven and grounded electrodes, this assumption is quite reasonable. In many other setups, the grounded and driven electrodes are located opposite each other and the electric field can, therefore, accelerate electrons also outside the capillary, making the electron-impact processes non-negligible there [9,10]. However, in geometries comparable to ours, it appears that the electrons lose most of their energy before exiting the capillary [11].

4. Results

The model results are compared with the biomedical experiments. In particular, photographs of the E.coli inactivation area are correlated against fluxes of various radicals to the substrate. Figure 2 shows the inactivation of the bacteria by a pure helium jet for the jet-substrate distance of 1.5 cm and the helium flow rate of 5.5 slm. Figure 3 shows fluxes of atomic oxygen, the hydroxyl radical and ozone to the substrate calculated for the same conditions.

Apparently, the fluxes of ozone and the hydroxyl radical to the Petri dish follow the ring shape that is observed in the experiment while the atomic oxygen flux does not. This follows from the fact that the atomic oxygen is produced through Penning ionization of oxygen and subsequent dissociative recombination early in the afterglow but it is very quickly converted to the hydroxyl radical and ozone, which are more stable.

5. References

[1] M. Laroussi, Plasma Process. Polym. **11**, 1138 (2014).

[2] D. B. Graves, Plasma Process. Polym. 11, 1120 (2014).

[3] N. Mericam-Bourdet et al, Journal of Physics D: Applied Physics, **42**, 2009.

[4] M. T. Madigan, J. M. Martinko, Biology of microorganisms. 11 ed, 2006, Upper Saddle River, NJ: Prentice Hall.

[5] C. R. Wilke, J. Chem. Phys. **18**, 517 (1950).

[6] T. Murakami, K. Niemi, T. Gans, D. O'Connell, and W. G. Graham, Plasma Sources Sci. Technol. **22**, 015003 (2013).

[7] M. Capitelli, C. M. Ferreira, B. F. Gordiets, and A. I. Osipov, Plasma Kinetics in Atmospheric Gases (Springer, Berlin, 2000), p. 300.

[8] K. Niemi, J. Waskoenig, N. Sadeghi, T. Gans, and D. O'Connell, **055005**, (2011).

[9] X. Y. Liu, X. K. Pei, X. P. Lu, and D. W. Liu, Plasma Sources Sci. Technol. **23**, 035007 (2014).

[10] G. V. Naidis, J. Appl. Phys. **112**, 103304 (2012).

[11] J. Jansky, Q. T. Algwari, D. O'Connell, and A. Bourdon, IEEE Trans. Plasma Sci. **40**, 2912 (2012).

6. Acknowledgements

A.O. is a Brno Ph.D. Talent Scholarship holder – funded by the Brno City Municipality. This work was supported by the project CEITEC - Central European Institute of Technology (CZ.1.05/1.1.00/02.0068) from European Regional Development Fund. K.A and S.P. would like to thank the U.S. Department of Energy Office of Science, Office of Basic Energy Sciences under Award Number DE-FC02-04ER15533